Electronic Supplementary Material (ESI) for Journal of Materials Chemistry A.

Remarkable Enhancement of the Electrochemical Properties of Co_3O_4 Nanowire Array by In Situ Surface Derivation of an Amorphous Phosphate Shell

Wenhui Li,[1] Mingyue Chen,[1] Wenhao Ma, Pengcheng Qi, Wanjun Yang, Shiyu Wang, Yu Lu and Yiwen Tang*

Institute of Nano-Science & Technology, College of Physical Science and Technology, Central China Normal University, Wuhan 430079, China
*Corresponding author: Tel.: +86-27-67867947; Fax: +86-27-67861185; E-mail: ywtang@mail.ccnu.edu.cn
[1]These authors contributed equally to this work

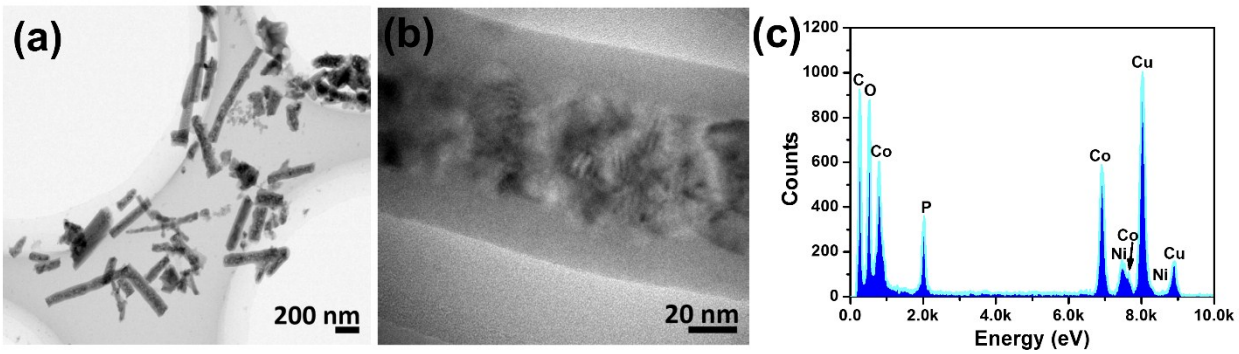

Fig S1. (a-b) Low and high magnification TEM images of Co_3O_4@Co-Pi, (c) EDS spectrum of Co_3O_4@Co-Pi.

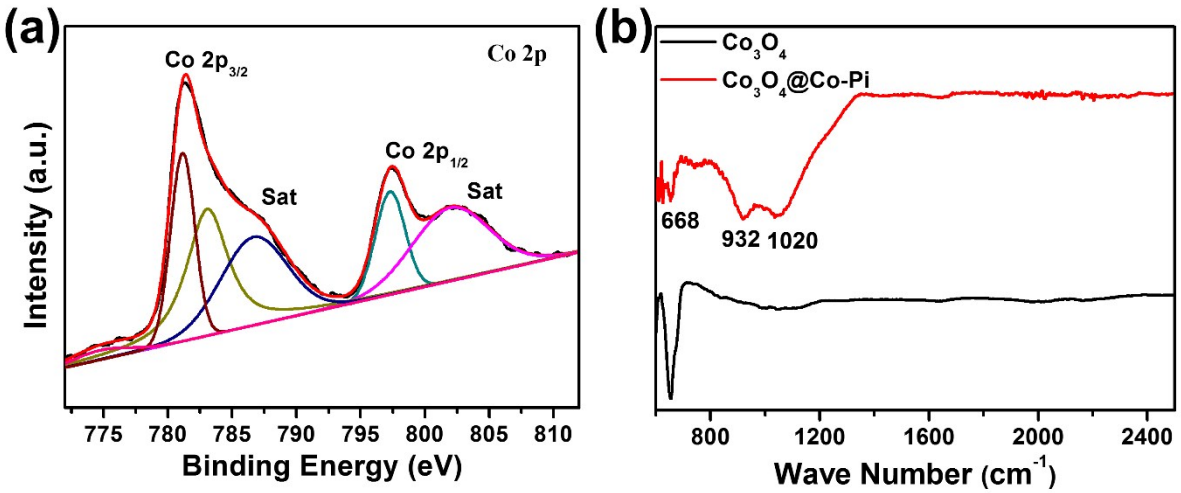

Fig S2. **(a)** XPS spectra of Co 2p for Co_3O_4. (b) FT-IR spectra of Co_3O_4 and Co_3O_4@Co-Pi.

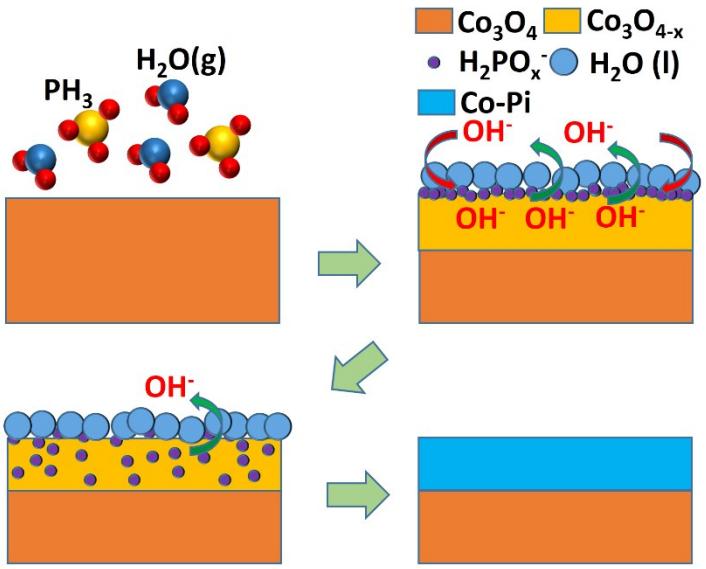

Fig S3. Illustration of the proposed morphology evolution mechanism of Co_3O_4@Co-Pi.

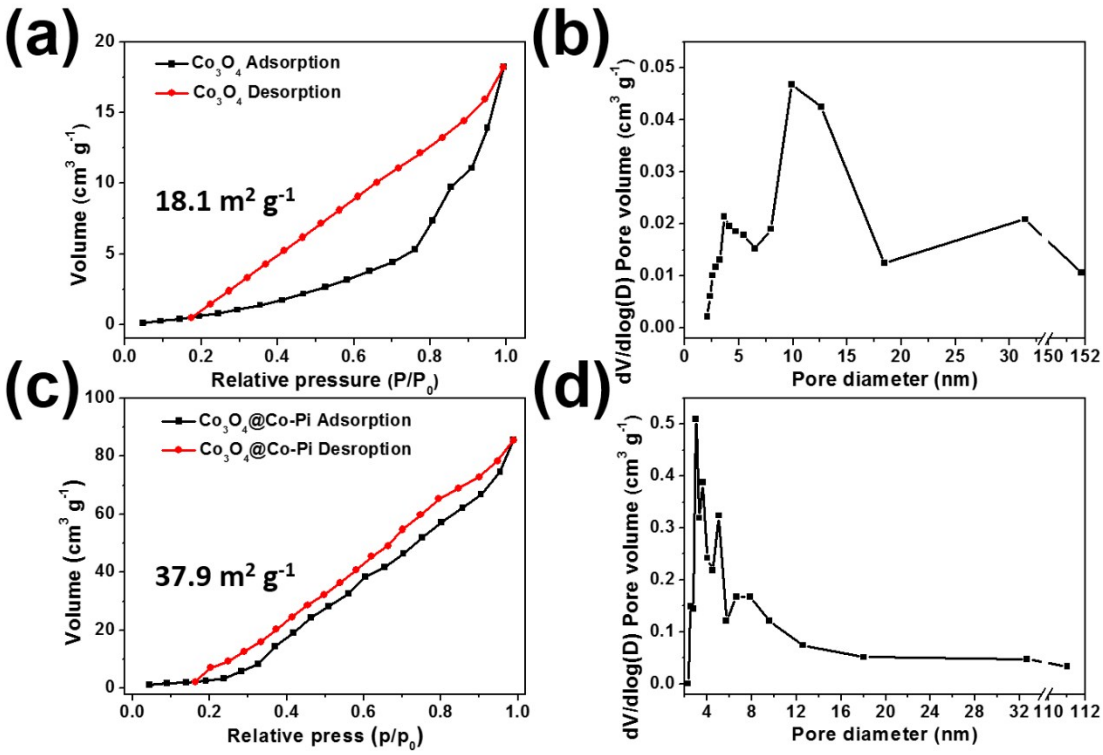

Fig S4. N_2 adsorption-desorption isotherms with the corresponding pore size distribution (a) and (b): Co_3O_4; (c) and (d): Co_3O_4@Co-Pi.

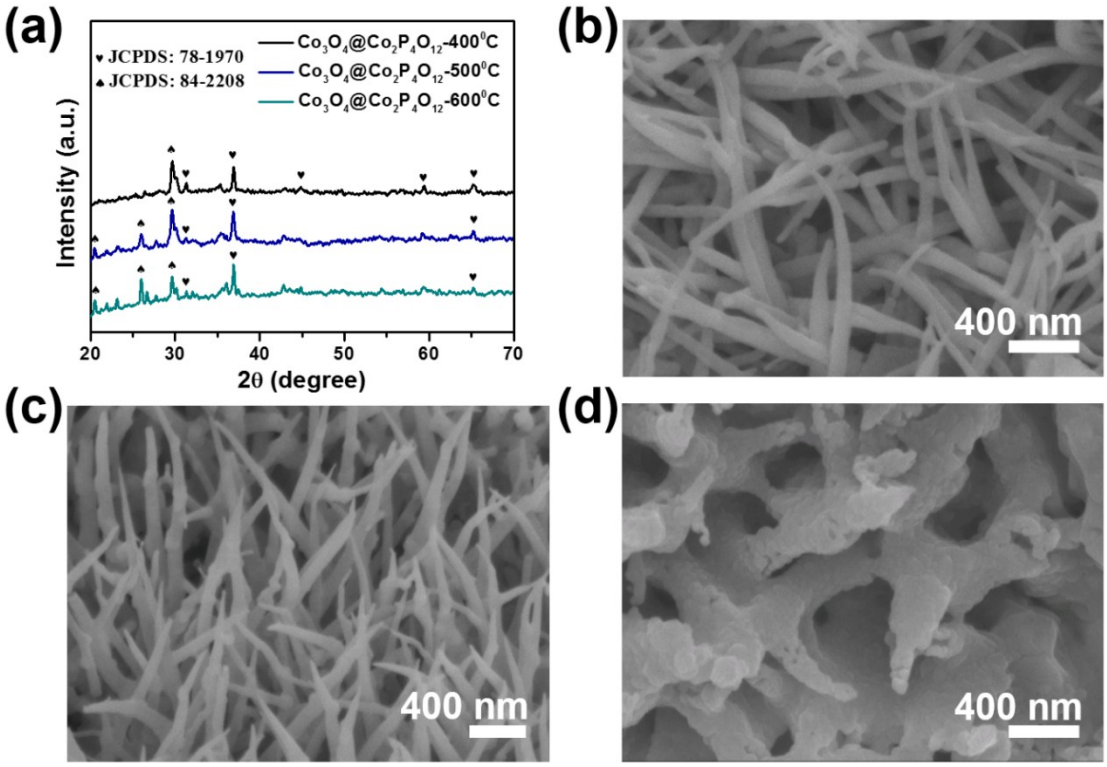

Fig S5. (a) XRD patterns of Co_3O_4@$Co_2P_4O_{12}$-400, Co_3O_4@$Co_2P_4O_{12}$-500, and Co_3O_4@$Co_2P_4O_{12}$-600 powders removed from the nickel foam. (b-d) SEM images of Co_3O_4@$Co_2P_4O_{12}$-400, Co_3O_4@$Co_2P_4O_{12}$-500 and Co_3O_4@$Co_2P_4O_{12}$-600.

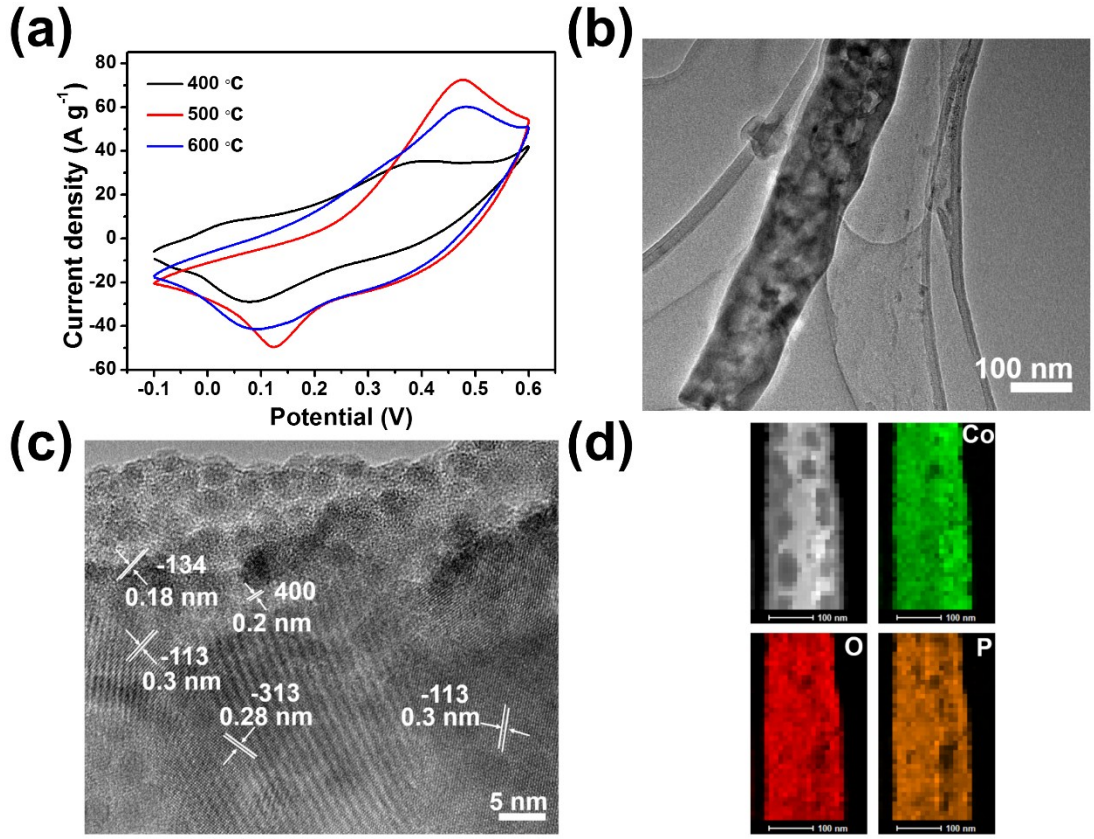

Fig S6. (a) CV curves of $Co_3O_4@Co_2P_4O_{12}$ electrode with different annealing temperature at 10 mV s^{-1}. (b-c) TEM image, HRTEM image $Co_3O_4@Co_2P_4O_{12}$-500. (d) Elemental mapping images of $Co_3O_4@Co_2P_4O_{12}$-500.

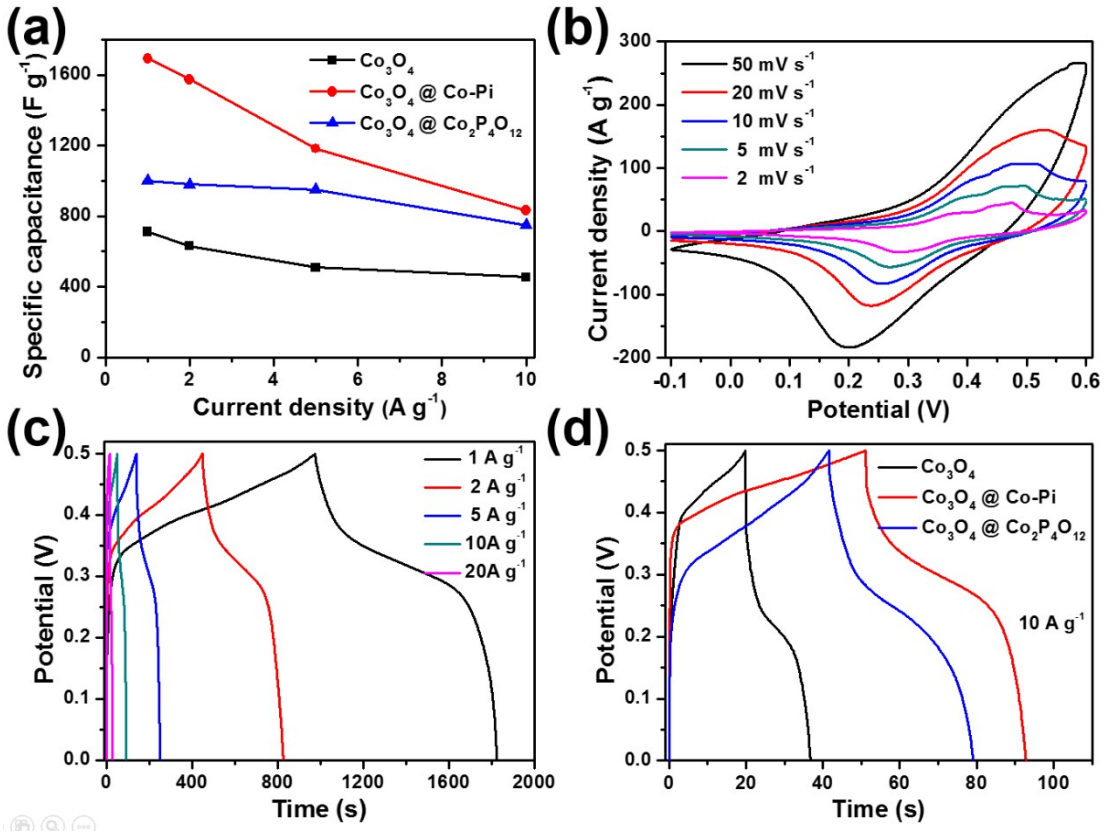

Fig S7. (a) Specific capacitance versus various current densities of Co_3O_4, Co_3O_4@Co-Pi, and Co_3O_4@$Co_2P_4O_{12}$. (b) CV curves of Co_3O_4@Co-Pi electrode collected at different scan rate. (c) GCD curves of Co_3O_4@Co-Pi electrode collected at different current density. (d) The voltage drop of three materials at a current density of 10 A g^{-1}.

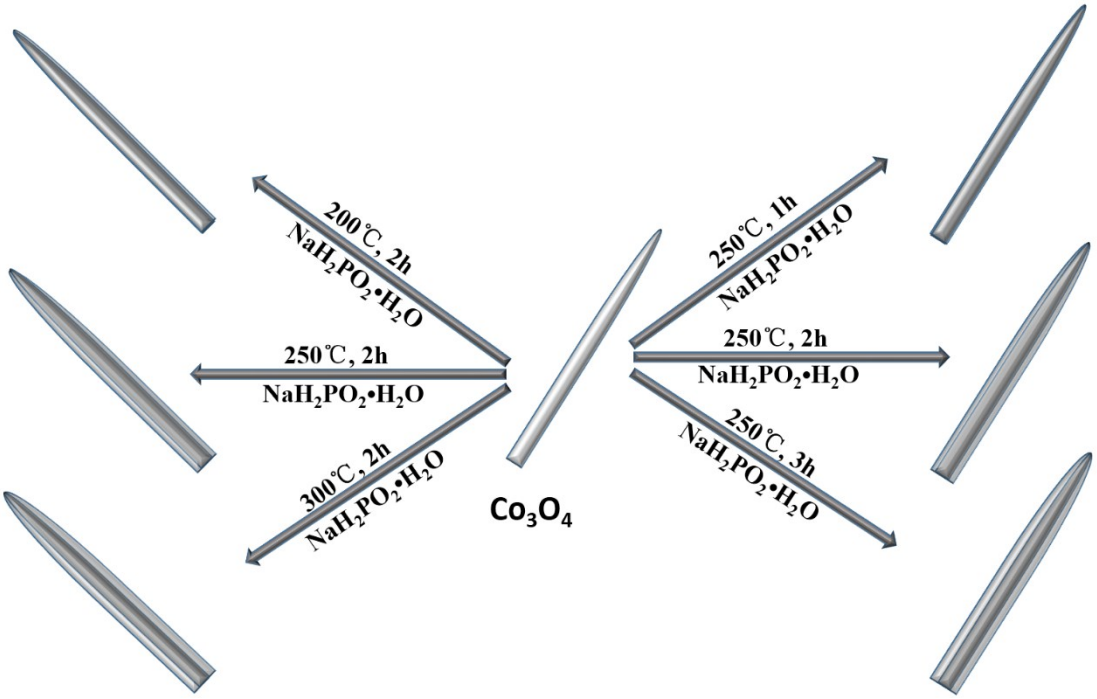

Fig S8. Schematic illustration of the phosphating process with different temperature and time for fabricating core-shell Co_3O_4@Co-Pi nanowires array.

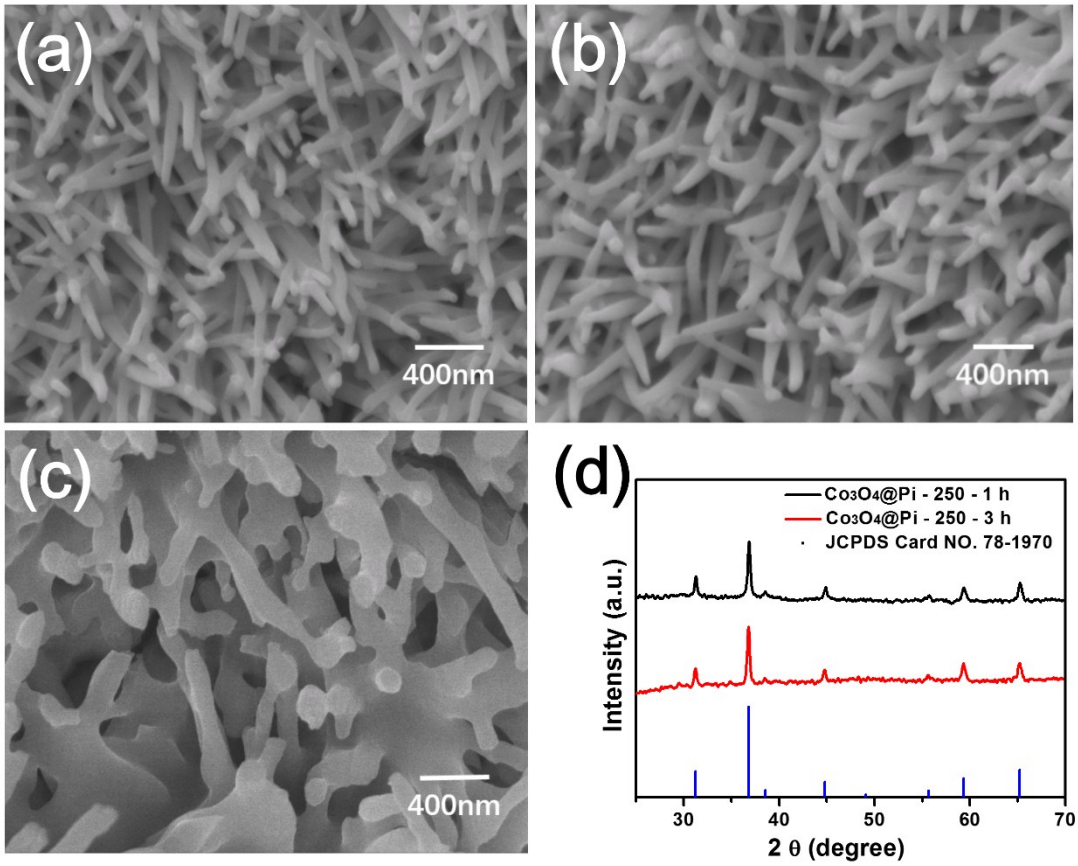

Fig S9. SEM images of Co_3O_4@Co-Pi with different phosphating time for 250 °C, (a) 1 h, (b) 2 h, (c) 3 h. (d) XRD patterns of Co_3O_4@Co-Pi prepared under 200 and 300°C, respectively, for 2 h.

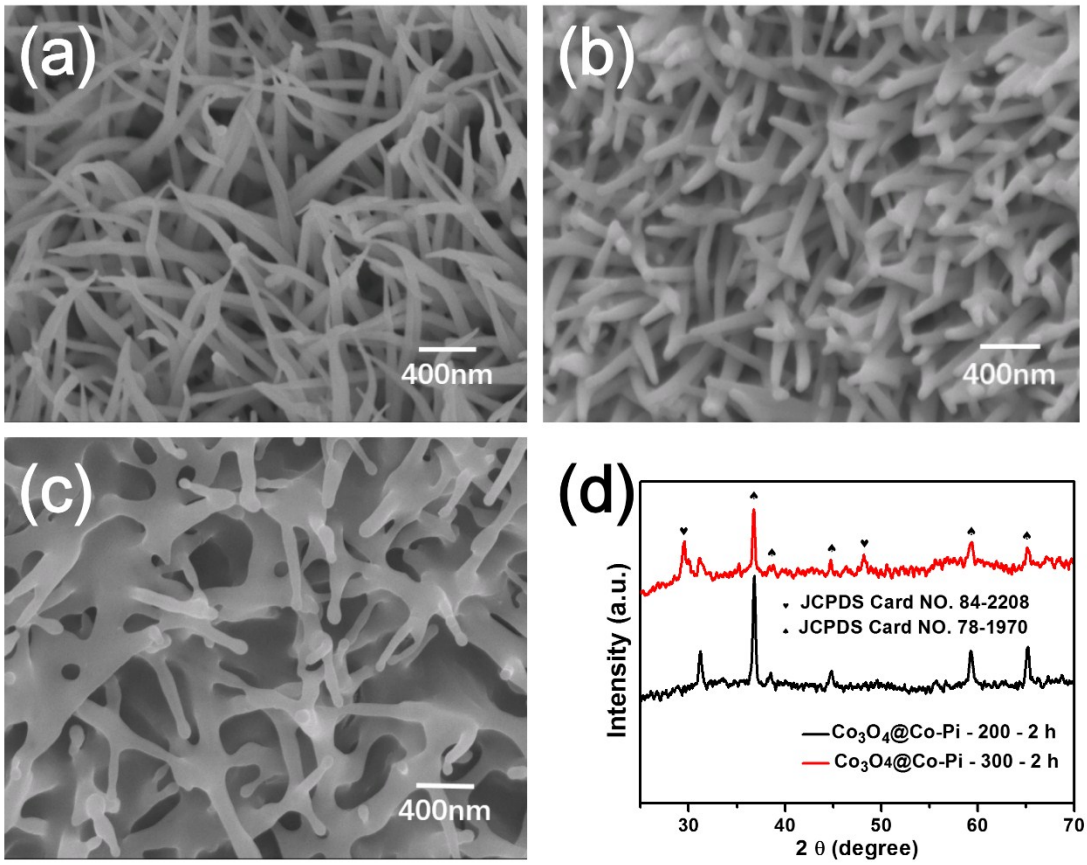

Fig S10. SEM images of Co_3O_4@Co-Pi with different phosphating temperature for 2 h: (a) 200°C; (b) 250°C; (c) 300°C. (d) XRD patterns of Co_3O_4@Co-Pi prepared under 200 and 300°C, respectively, for 2 h.

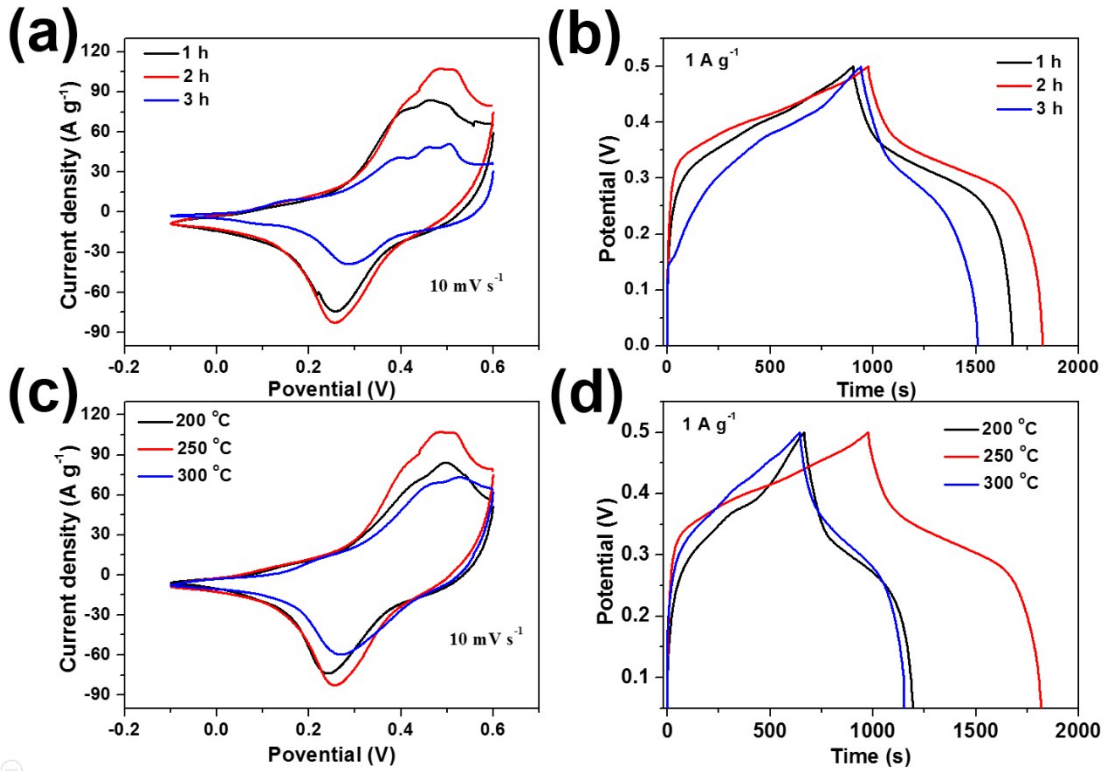

Fig S11. Electrochemical characterization of Co_3O_4@Co-Pi: (a) CV curves of different phosphating time; (b) GCD plots; (c) CV curves of different phosphating temperature; (d) GCD plots.

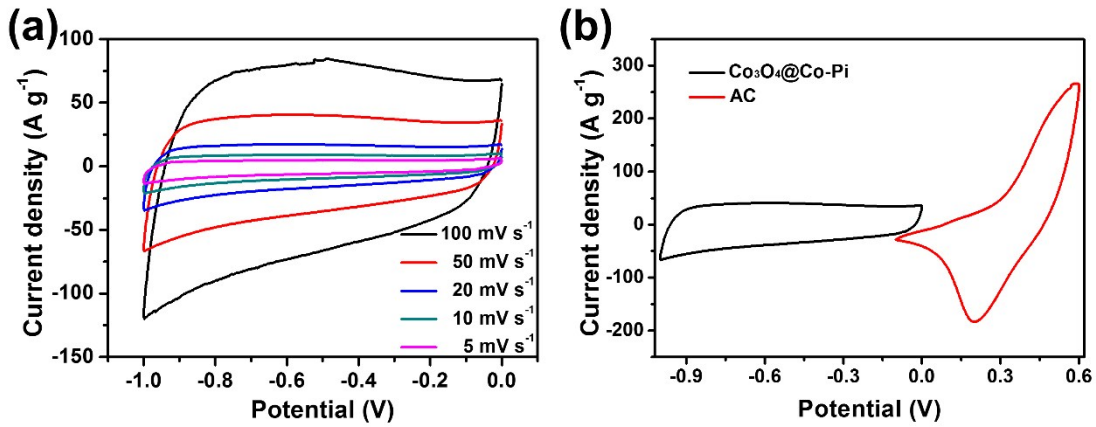

Fig S12. (a) CV curves of activated carbon. (b) CV curves at 50 mV/s of Co_3O_4@Co-Pi//AC supercapacitor.

Table S1. Electrochemical performance obtained from Co_3O_4 based electrodes.

Type of electrode	Specific (areal) capacitance	Rate capability	Capacitance retention	Ref.
Co_3O_4@Co-Pi core–shell hybrid nanostructure	1692 F g^{-1} at of 1 A g^{-1}	56.1% from 1 to 10 A g^{-1}	86% after 6,000 cycles	This work
RuO_2/Co_3O_4 nanosheets	905 F g^{-1} at 1 A g^{-1}	78% from 1 to 40 A g^{-1}	96% after 5,000 cycles	[1]
layered Co_3O_4	265 F g^{-1} at 1 A g^{-1}	64.6% from 1 to 6 A g^{-1}	89.6% after 1,000 cycles	[2]
Co_3O_4 nanowires	746 F g^{-1} at 0.6 A g^{-1}	No data	86% after 500 cycles	[3]
α-$Co(OH)_2/Co_3O_4$ nanorods	583 F g^{-1} at 1 A g^{-1}	No data	No obvious specific capacitance loss after 2000 cycles	[4]
Co_3O_4@MnO_2	560 F g^{-1} at 0.2 A g^{-1}	54.5% from 0.2 to 10 A g^{-1}	No negligible	[5]
Co_3O_4 nanoparticles	370 F g^{-1} at 0.5 A g^{-1}	No data	No negligible	[6]
plate-like Co_3O_4	393.6 F g^{-1} at 1 A g^{-1}	No data	96.5% after 500 cycles	[7]
ultralayered Co_3O_4	548 F g^{-1} at 4 A g^{-1}	59.4% from 4 to 32 A g^{-1}	98.5% after 2000 cycles	[8]
Hollow Co_3O_4 nanowire arrays	599 F g^{-1} at 2 A g^{-1}	73.3% from 2 to 40 A g^{-1}	No negligible	[9]
Co_3O_4/GO	157.7 F g^{-1} at 0.1 A g^{-1}	51.8% from 0.1 to 2 A g^{-1}	70% after 4000 cycles	[10]
flower-like NiO-Co_3O_4	1190 F g^{-1} at 4 A g^{-1}	No data	99% after 5000 cycles	[11]
PCO NWAs	1716 F g^{-1} at 5 mV s^{-1}	No negligible	85% after 1,0000 cycles	[12]

References:

[1] Rakhi, R.B., Chen, W.; Hedhili, M. N.; Cha, D.; Alshareef, H. N., *ACS Appl. Mater. Interface* **2014**, *6*, 4196.

[2] Xie, L., Li, K.; Sun, G.; Hu, Z.; Lv, C.; Wang, J.; Zhang, C., *J. Solid State Electr.*

2013, *17*, 55.

[3] Gao, Y., Chen, S.; Cao, D.; Wang, G.; Yin, J., *J. Power Sources* **2010**, *195*, 1757.

[4] Jing, M., Yang, Y.; Zhu, Y.; Hou, H.; Wu, Z.; Ji, X., *Electrochim. Acta* **2014**, *141*, 234.

[5] Huang, M., Zhang, Y.; Li, F.; Zhang, L.; Wen, Z.; Liu, Q., *J. Power Sources* **2014**, *252*, 98.

[6] Xia, X.-h.; Tu, J.-p.; Zhang, Y.-q.; Mai, Y.-j.; Wang, X.-l.; Gu, C.-d.; Zhao, X.-b., *Rsc Adv.* **2012**, *2*, 1835.

[7] Aghazadeh, M., *J. Appl. Electrochem.* **2012**, *42*, 89.

[8] Meher, S. K.; Rao, G. R., *J. Phys. Chem. C* **2011**, *115*, 15646.

[9] Xia, X.-h.; Tu, J.-p.; Mai, Y.-j.; Wang, X.-l.; Gu, C.-d.; Zhao, X.-b., *J. Mater. Chem.* **2011**, *21*, 9319.

[10] Q. Guan, J. Cheng, B. Wang, W. Ni, G. Gu, X. Li, L. Huang, G. Yang, F. Nie, *ACS Appl. Mater. Interface* **2014**, *6*, 7626.

[11] Xu, K.; Zou, R.; Li, W.; Xue, Y.; Song, G.; Liu, Q.; Liu, X.; Hu, J., *J. Mater. Chem. A* **2013**, *1*, 9107.

[12] Zhai, T.; Wan, L.; Sun, S.; Chen, Q.; Sun, J.; Xia, Q.; Xia, H., *Adv. Mater.* **2017**, *29*.